PAPER • OPEN ACCESS

Chemical short-range order in liquid Ni–Cu

To cite this article: Dirk Holland-Moritz *et al* 2023 *J. Phys.: Condens. Matter* **35** 465403

View the article online for updates and enhancements.

You may also like

- Observed and simulated local climate responses to tropical deforestation
Callum Smith, Jessica C.A. Baker, Eddy Robertson et al.

- Spatiotemporal Denoising of Low-dose Cardiac CT Image Sequences using RecycleGAN
Shiwei Zhou, Jinyu Yang, Krishnateja Konduri et al.

- CNT incorporation improves the resolution and stability of porous 3D printed PLGA/HA/CNT scaffolds for bone regeneration
Hatice Kaya, ule Arc, Osman Bulut et al.

Chemical short-range order in liquid Ni–Cu

Dirk Holland-Moritz[1,]* , **Fan Yang[1]** , **Thomas C Hansen[2]** and **Florian Kargl[1]**

[1] Institut für Materialphysik im Weltraum, Deutsches Zentrum für Luft- und Raumfahrt, 51170 Köln, Germany
[2] Institut Laue-Langevin (ILL), 38042 Grenoble, France

E-mail: dirk.holland-moritz@dlr.de

CrossMark

Abstract
Neutron diffraction in combination with isotopic substitution on the zero-scatterer $^{62}Ni_{43}^{63}Cu_{57}$ shows indications for chemical short-range order in the stable liquid as evidenced by oscillations in the concentration–concentration structure factor $S_{CC}(q)$. This points towards a non-ideal solution behavior of Ni–Cu contrary to common believe but in agreement with measurements of free enthalpy of mixing. The temperature dependence of S_{CC} at small momentum transfer provides evidence of critical compositional fluctuations in $Ni_{43}Cu_{57}$ melts.

Keywords: short-range order of liquids, demixing, neutron diffraction

(Some figures may appear in colour only in the online journal)

1. Introduction

Critical behavior in liquids has been studied for a large number of systems so far: amongst those are water [1, 2], molecular liquids [3], oxide melts [4], and metallic melts [5–8]. In general critical phenomena recently received renewed interest. Two kinds of phase separation can hereby be distinguished: physical phase separation and chemical phase separation. The former is typically associated with a change in density like recently reported for example for Y_2O_3–Al_2O_3 liquids [4], phosphorous [9] or amorphous ice [10, 11], whereby the system remains chemically homogeneous but separates into a denser and a less dense phase. Chemical phase separation on the other hand is associated with separation into two chemically different phases. For the metallic liquid Cu–Co, which

shows a rich phase diagram it has been shown that Cu and Co demix if the liquid is supercooled below its metastable binodal line [5, 6]. In contrast Ni–Cu, with Ni being the neighboring element to Cu in the periodic table, shows a comparatively simple phase diagram of a solid solution. Taken its lens-shaped two phase regime between liquidus and solidus line, the Ni–Cu system on first sight might be considered as a typical representative of a next to ideal solution. Studies at lower temperatures in the solid, however, are indicative of clustering in the alloy [12, 13]. Moreover, thermodynamic assessments predict a miscibility gap to occur deep in the solid [14–16]. There remains controversy about the critical temperature of the miscibility gap. A direct experimental investigation of this miscibility gap using classical methods is impossible due to the very low diffusivities in solid state at the relevant temperatures, resulting to required time frames beyond feasibility. Most observations and thermodynamic assessments suggest that the critical temperature is located around 600 K [13]. Moreover, the critical point is shifted to the more Ni-rich side of the phase diagram.

Clustering in solid state that was reported to occur in solid Ni–Cu alloys means that the different types of atoms are not randomly distributed on the crystal lattice but show

compositional fluctuations. Liquids are characterized by an absence of a long-range topological order such that there exists only a short-range topological order. Nevertheless, fluctuations of the chemical composition or even chemical decomposition on macroscopic length scales [5, 6] are not tied to a long-range topological order but may also be observed for liquid systems.

In the liquid state (including the regime of undercooled melts) measurements of the electrical resistivity on Ni–Cu alloys show a non-linear temperature dependence for the Cu-rich alloys $Ni_{40}Cu_{60}$ and $Ni_{20}Cu_{80}$, while for Ni-rich alloys the usual linear temperature dependence is observed [17]. The deviation from linearity might indicate a demixing behavior that increases with increasing undercooling of the liquids. The local density fluctuations associated with the demixing may give rise to scattering of the conduction electrons resulting to an increase of the electrical resistivity [18, 19]. Also the positive enthalpy of mixing [20], points towards a demixing nature of this system. However, the enthalpy of mixing for Ni–Cu is only slightly positive compared with the enthalpy of mixing of Cu–Co. Hence, the demixing behavior of Ni–Cu is expected to be not as clearly pronounced as for the Cu–Co system and therefore might have been unaccounted for in previous investigations which were also not specifically tailored to this task.

Interestingly the generic behavior of phase separation has recently been studied by means of molecular dynamics simulations on binary symmetric Lennard–Jones mixtures of A and B atoms [21, 22]. Here the interaction potentials are given by

$$V_{\alpha\beta}(r) = 4\varepsilon_{\alpha\beta} \left\{ \left(\frac{\sigma_{\alpha\beta}}{r} \right)^{12} - \gamma \left(\frac{\sigma_{\alpha\beta}}{r} \right)^{6} \right\}, \qquad (1)$$

where r denotes the distance between the atoms of type α and β, and $\varepsilon_{\alpha\beta}$, $\sigma_{\alpha\beta}$ and γ are parameters. In [21, 22] $\sigma_{AB} = \sigma_{AA} = \sigma_{BB} = \sigma$ and $\varepsilon_{AA} = \varepsilon_{BB} = \varepsilon$ was chosen. For $\gamma \geqslant 1$, which corresponds to attractive interactions, a demixing behavior has been found upon cooling, if the interaction parameters $\varepsilon_{\alpha\beta}$ of the unlike atomic pairs are smaller than those of the like atomic pairs ($\varepsilon_{AB} < \varepsilon = \varepsilon_{AA} = \varepsilon_{BB}$), or in other words if the potential minima are deeper for like atomic pairs than for unlike pairs. For a real system, depending on the shape of the real interaction potentials, the critical point might not be exactly at the 50:50 composition and the spinodal line might be slightly skewed. Nonetheless this generic behavior should occur also in real liquids.

It is important to note that a critical behavior and therefore a corresponding rise in the concentration–concentration partial structure factor $S_{CC}(q)$ will not be restricted to the critical point only [8]. The critical behavior as determined for instance by a critical rise in this structure factor will extend sufficiently far into phase-space. Therefore critical fluctuations will be visible already well above the critical point. This shall be visible by a rise in $S_{CC}(q)$ at low-q values. Hence, a study of liquid Ni–Cu is expected to reveal critical fluctuations already at the melting temperature.

Table 1. Scattering lengths b of the isotopes used to prepare the alloys.

|	^{nat}Cu	^{63}Cu	^{nat}Ni	^{58}Ni	^{60}Ni	^{62}Ni
b (fm)	7.718	6.43	10.3	14.4	2.8	−8,7

2. Experimental

In order to study the short-range order of liquid Ni–Cu alloys, neutron diffraction experiments were performed on the D20 diffractometer at the Institute Laue-Langevin, Grenoble, France. An electromagnetic levitation (EML) device was used as sample environment. The EML was already described previously [23]. Here, we only highlight that by using this sample environment not only supercooling of a liquid below its liquidus temperature due to the absence of container walls is possible, but also the signal-to-background ratio in scattering experiments is excellent. Considering the high melting point and chemical reactivity Ni–Cu cannot be processed in a vanadium container otherwise used for neutron diffraction experiments. D20 was chosen since due to its high-flux it proved in the past ideal for measuring partial structure factors of isotopically-substituted small spherical-shaped samples with excellent statistics within a short period of time [24–27].

The experiments discussed here were performed on 6–8 mm diameter spheres of $Ni_{42.7}Cu_{57.3}$. A total of four samples with different isotope mixtures were investigated. This particular sample composition was chosen to enable, by mixing of the pure ^{62}Ni with the pure ^{63}Cu isotope, the synthesis of a so-called zero-scattering alloy. For such an alloy the mean value of the scattering length is zero: $\bar{b} = c_A b_A + c_B b_B = 0$, where c_A and c_B are the compositions of the alloy components A and B and b_B and b_B their coherent scattering lengths. This is the case due to the negative scattering length of ^{62}Ni and the positive scattering length of ^{63}Cu (see table 1). As discussed below, the advantage of a zero scattering alloy is that in Bathia–Thornton notation [19] the contribution of the number–number $S_{NN}(q)$ and the number-concentration $S_{NC}(q)$ structure factors to the total structure factor $S(q)$ vanish and $S_{CC}(q)$ can be directly measured [8, 28, 29]. Moreover, scattering experiments were performed on mixtures of ^{nat}Ni, ^{60}Ni, and ^{58}Ni with natural copper, respectively. It should also be stressed that the $Ni_{42.7}Cu_{57.3}$ composition is close to the $Ni_{40}Cu_{60}$ composition for which a strongly non-linear temperature dependence of the electrical resistivity has been reported [17]. For comparison also neutron diffraction measurements on pure Cu have been performed.

3. Results and discussion

For an analysis of the short-range order in a binary A–B melt, partial static structure factors may be calculated from three independent total static structure factors according to the Bhatia–Thornton [19] or the Faber–Ziman formalism [30]. Bhatia and Thornton have defined three partial static structure factors: $S_{NN}(q)$ describes the topological short-range order of the liquid, $S_{CC}(q)$ the chemical short-range order, and $S_{NC}(q)$
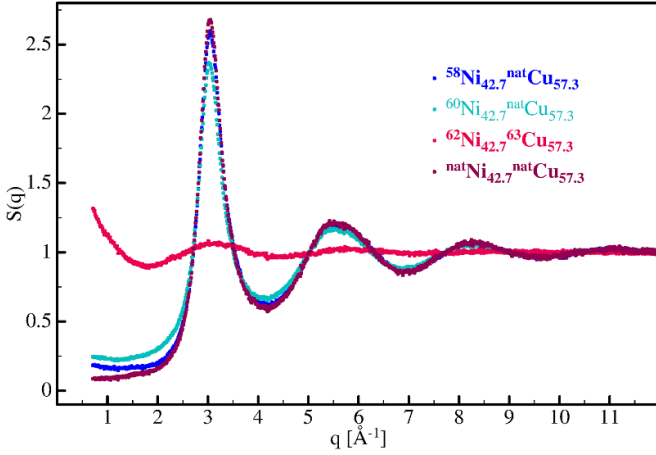
Figure 1. Total structure factors of $Ni_{42.7}Cu_{57.3}$ of different isotopic composition at the liquidus temperature of $T_L = 1560$ K.

Figure 2. Bhatia–Thornton structure factors S_{NN} (blue symbols), S_{CC} (red symbols) and S_{NC} (green symbols) of liquid $Ni_{42.7}Cu_{57.3}$ at the liquidus temperature of $T_L = 1560$ K determined from the three total structure factors measured by neutron scattering on samples of the isotopic compositions $^{58}Ni_{42.7}{}^{nat}Cu_{57.3}$, $^{60}Ni_{42.7}{}^{nat}Cu_{57.3}$ and $^{62}Ni_{42.7}{}^{63}Cu_{57.3}$. Under these scattering contrast conditions S_{CC} is directly given by the total structure factor of the zero-scattering alloy $^{62}Ni_{42.7}{}^{63}Cu_{57.3}$. Also shown is S_{CC} inferred from the total structure factors measured for samples of $^{58}Ni_{42.7}{}^{nat}Cu_{57.3}$, $^{60}Ni_{42.7}{}^{nat}Cu_{57.3}$ and $^{nat}Ni_{42.7}{}^{nat}Cu_{57.3}$ (gray symbols). The S_{NN} and S_{NC} calculated from the latter set of data can hardly be distinguished from the ones determined from the former set of data and they are therefore not shown.

the correlation of number density and chemical composition. The relation between the total structure factors and the partial Bhatia–Thornton structure factors is given by:

$$S(q)^{BT} = \frac{\overline{b}^2}{\overline{b^2}}S_{NN} + \frac{c_A c_B (b_A - b_B)^2}{\overline{b^2}}S_{CC} + \frac{2(b_A - b_B)\overline{b}}{\overline{b^2}}S_{NC}.$$

(2)

c_A and c_B denote the concentrations of the atoms of type A and B in the melt, b_A and b_B are the coherent scattering lengths of the atoms/isotopes, $\overline{b} = c_A b_A + c_B b_B$ and $\overline{b^2} = c_A b_A{}^2 + c_B b_B{}^2$.
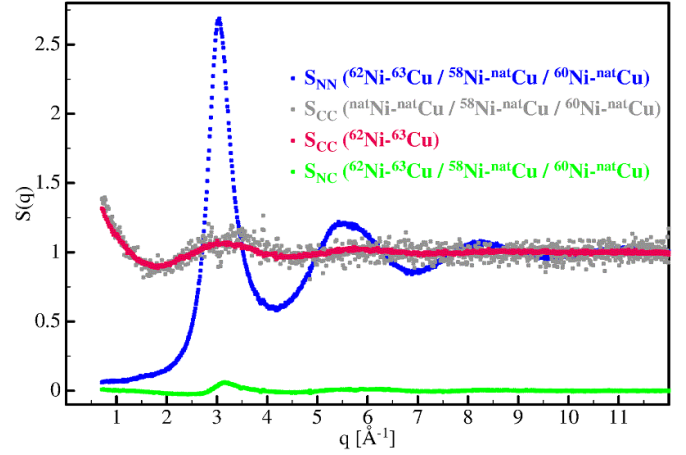
In the framework of the Faber–Ziman formalism the three partial static structure factors $S_{AA}(q)$, $S_{BB}(q)$, and $S_{AB}(q)$ describe the contributions to the total structure factor $S(q)$ that result from correlations between the three different types of pairs of atoms (A–A, B–B, and A–B):

$$S(q)^{FZ} = \frac{c_A^2 b_A{}^2}{\overline{b^2}}S_{AA} + \frac{c_B^2 b_B{}^2}{\overline{b^2}}S_{BB} + \frac{2c_A c_B b_A b_B}{\overline{b^2}}S_{AB} + 1 - \frac{\overline{b}^2}{\overline{b^2}}.$$

(3)

The total structure factors $S(q)$ of $^{62}Ni_{42.7}{}^{63}Cu_{57.3}$, $^{58}Ni_{42.7}{}^{nat}Cu_{57.3}$, $^{60}Ni_{42.7}{}^{nat}Cu_{57.3}$ and $^{nat}Ni_{42.7}{}^{nat}Cu_{57.3}$ melts measured at the liquidus temperature $T_L = 1560$ K are shown in figure 1.

Because the largest scattering contrast is obtained between the measurements on the $^{62}Ni_{42.7}{}^{63}Cu_{57.3}$, $^{58}Ni_{42.7}{}^{nat}Cu_{57.3}$ and $^{60}Ni_{42.7}{}^{nat}Cu_{57.3}$ sample, this set of data has been used in order to determine partial structure factors within the Bhatia–Thornton [19] and the Faber–Ziman [30] formalism.

The corresponding Bhatia–Thornton structure factors after matrix-inversion are shown in figure 2, the Faber–Ziman structure factors in figure 3. Because for a zero-scattering alloy $\overline{b} = c_A b_A + c_B b_B = 0$, the prefactors of S_{NN} and S_{NC} in equation (2) vanish and S_{CC} and the total structure factor measured for the zero-scattering alloy are identical. For S_{CC} a rise in intensity is observed at low-q on top of a relatively large flat background with some smaller oscillations towards larger q-values. It directly points to the demixing nature of the system with concentration fluctuations on larger than atomic

length scales. The comparatively weak demixing behavior is evidenced by the small oscillations in S_{CC} towards larger q-values. While the rise at low-q is pronounced in the total structure factor measured for the zero-scattering alloy, it is not immediately apparent in the total structure factors of the other isotope compositions. Here, one has to bear in mind that the S_{CC} contribution to each of these total structure factors is only weakly pronounced. In order to rule out that the rise at low q is an artifact in the measurement on $^{62}Ni_{42.7}{}^{63}Cu_{57.3}$ resulting for instance from an incomplete subtraction of the background at small angles close to the primary beam, we have calculated S_{CC} also from the set of total structure factors given by $^{58}Ni_{42.7}{}^{nat}Cu_{57.3}$, $^{60}Ni_{42.7}{}^{nat}Cu_{57.3}$ and $^{nat}Ni_{42.7}{}^{nat}Cu_{57.3}$. As shown in figure 2, the result is in good agreement with the structure factor of the zero-scattering alloy, confirming that the rise of S_{CC} to low q reflects intrinsic properties of the alloy. The larger scatter in the data can be explained being due to the small differences of the measured total structure factors for the three different isotope mixtures. The S_{NN} and S_{NC} calculated from the latter set of data can hardly be distinguished from the ones determined from the former set of data and are therefore not shown.

It is remarkable that the shapes of the measured Bhatia–Thornton partial structure factors closely resemble those that have previously been reported for binary Lenard–Jones mixtures [21, 22] for the case that in the simulations the interaction parameters $\varepsilon_{\alpha\beta}$ of the unlike atomic pairs are smaller than those of the like atomic pairs. Moreover, for this case and if the parameter λ that is a weight of the attractive term in the
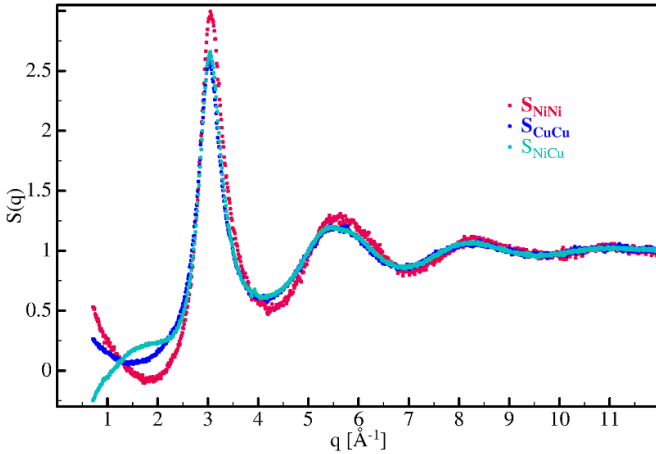
Figure 3. Faber–Ziman structure factors S_{NiNi} (red symbols), S_{CuCu} (blue symbols) and S_{NiCu} (cyan symbols) of liquid $Ni_{42.7}Cu_{57.3}$ at the liquidus temperature of $T_L = 1560$ K determined from the three total structure factors measured by neutron scattering on samples of the isotopic compositions $^{58}Ni_{42.7}{}^{nat}Cu_{57.3}$, $^{60}Ni_{42.7}{}^{nat}Cu_{57.3}$ and $^{62}Ni_{42.7}{}^{63}Cu_{57.3}$.
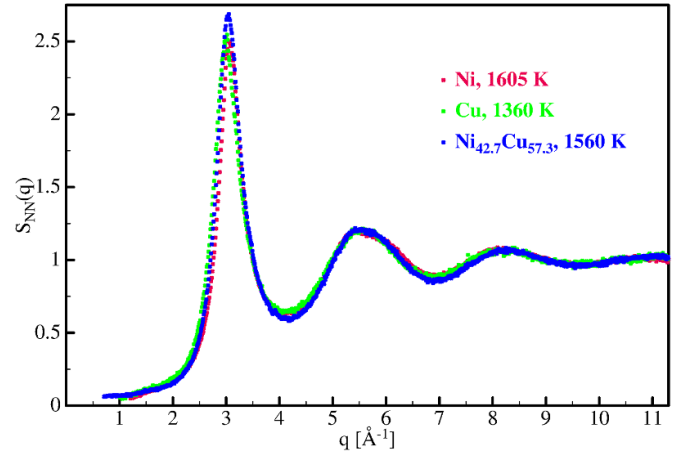

Figure 4. Comparison of the number–number structure factor S_{NN} of liquid $Ni_{42.7}Cu_{57.3}$ at the liquidus temperature of $T_L = 1560$ K with the structure factors of pure liquid Ni [32] at $T = 1605$ K and pure liquid Cu at $T = 1360$ K.

potential is not too large, the MD-simulations also reproduce other characteristic properties of the Ni–Cu system like the positive enthalpy of mixing and the negative excess volume [31]. Obviously, main predictions on the dependence of the chemical short-range order and of thermophysical properties on the atomic interactions inferred from this simple generic model are found in real metallic systems like Cu–Ni.

The Bhatia–Thornton partial structure factor S_{NN} describes the topological short-range order of the melt. In figure 4 it is compared with the structure factor of pure liquid Cu at $T = 1360$ K also measured as part of this work and with that of pure Ni at $T = 1605$ K as published in [32]. All structure factors have a similar shape and show a characteristic shoulder on the right side of the second oscillation that is usually considered as an indication of an icosahedral topological short-range order [32, 33].

Within the Faber–Ziman formalism the partial structure factors S_{NiNi}, S_{CuCu} and S_{NiCu} describe the contributions of the different pairs of atoms (Ni–Ni, Cu–Cu and Ni–Cu) to the total structure factor. Despite similarities in their shape, subtle differences are evident in figure 3, again indicating some degree of chemical short-range order, because in the case of a chemically fully disordered system all Faber–Ziman structure factors and also S_{NN} would be identical [19].

The partial pair correlation functions, $g_{NN}(r)$, $g_{CC}(r)$, $g_{NC}(r)$, $g_{NiNi}(r)$, $g_{NiCu}(r)$, and $g_{CuCu}(r)$ are calculated by Fourier transformation from the partial static structure factors. These are shown in figure 5. The positions of the first maxima of $g_{NN}(r)$, $g_{NiNi}(r)$, $g_{CuCu}(r)$, and $g_{NiCu}(r)$ correspond to the nearest neighbor distances for the different types of atomic pairs. These are compiled in table 2. All mean nearest neighbor distances determined for the $Ni_{42.7}Cu_{57.3}$ alloy are slightly shorter as those of the pure elements, which may provide a structural explanation of the reported negative excess volume [31]. This shrinkage of the interatomic distances
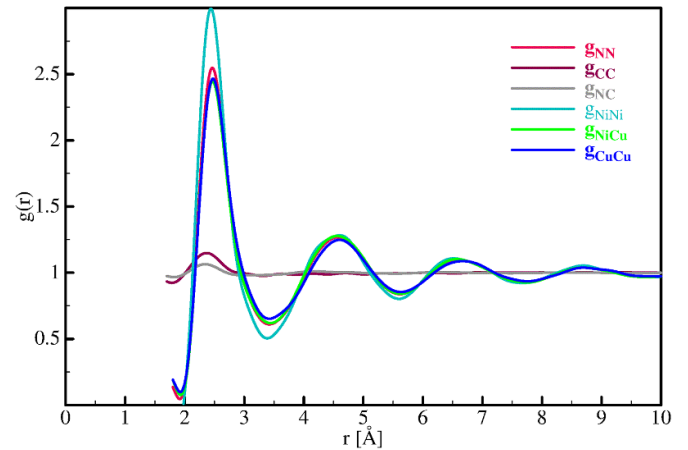

Figure 5. Partial pair correlation functions of liquid $Ni_{42.7}Cu_{57.3}$ at the liquidus temperature of $T_L = 1560$ K.

appears most pronounced for the Ni–Ni nearest neighbor pairs. A similar preferred reduction of one type of nearest neighbor pairs was recently reported in molecular-dynamics simulations of liquid Al–Au alloys [34]. Table 2 also gives the partial nearest neighbor coordination numbers, Z_{NN}, Z_{NiNi}, Z_{NiCu} and Z_{CuCu} as well as the averaged coordination number $<Z> = c_{Ni}(Z_{NiNi} + Z_{CuNi}) + c_{Cu}(Z_{CuCu} + Z_{NiCu})$, where c_{Ni} and c_{Cu} are the concentrations of Ni and Cu in the alloy. The partial coordination numbers are calculated by integrating the first peak of the partial radial distribution function $4\pi c_B \rho_N r^2 g_{AB}(r)$ (A, B = N, Ni, Cu) between its first and second minimum. Here ρ_N denotes the number density. Here we use a value of $\rho_N = 0.08$ at. Å^{-3}, which is inferred from the density of a $Cu_{60}Ni_{40}$ alloy melt of close composition at its melting temperature [35]. Z_{NN} that is calculated from the Bhatia–Thornton structure factor S_{NN} is in good agreement with $<Z>$ that is determined from the Faber–Ziman partial structure factors. The minor deviation is due to the errors in the determination of the different partial coordination numbers

Table 2. Distances of atomic nearest neighbors (d_{NN}, d_{NiNi}, d_{CuCu} and d_{NiCu}) and partial nearest neighbor coordination numbers (Z_{NN}, Z_{NiNi}, Z_{CuCu}, Z_{NiCu} and Z_{CuNi}) for melts of $Ni_{42.7}Cu_{57.3}$ and of the pure elements Ni [32] and Cu.

	$Ni_{42.7}Cu_{57.3}$	Ni	Cu
T (K)	1560	1605	1356
d_{NN} (Å)	2.46 ± 0.02	2.49 ± 0.02	2.48 ± 0.02
d_{NiNi} (Å)	2.44 ± 0.02	2.49 ± 0.02	
d_{CuCu} (Å)	2.47 ± 0.02		2.48 ± 0.02
d_{NiCu} (Å)	2.47 ± 0.02		
Z_{NN}	12.6 ± 0.5	11.9 ± 0.5	12.5 ± 0.5
Z_{NiNi}	5.7 ± 0.5	11.9 ± 0.5	
Z_{CuCu}	7.2 ± 0.5		12.5 ± 0.5
Z_{NiCu}	5.2 ± 0.5		
Z_{CuNi}	7.0 ± 0.5		
$<Z>$	12.5 ± 0.5	11.9 ± 0.5	12.5 ± 0.5
Reference	This work	[32]	This work
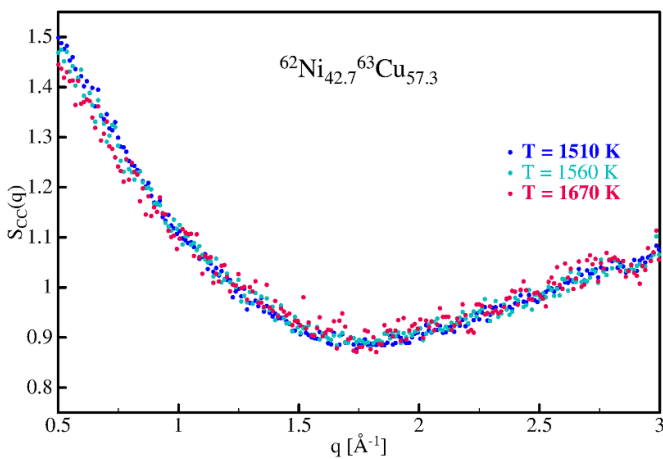
Figure 6. Temperature dependence of the concentration–concentration structure factor S_{CC} of liquid $Ni_{42.7}Cu_{57}$ at small momentum transfer q.

(including those due to the Fourier transformation when calculating the pair correlation functions from the structure factors).

The partial structure factors discussed before have been measured at the melting temperature of the $Ni_{42.7}Cu_{57.3}$ alloy providing clear evidence of a demixing behavior even at this elevated temperature and showing the characteristic increase of S_{CC} at small q. Inspired by this finding we performed investigations on the temperature dependence of the increase of S_{CC} at small momentum transfer, aiming to study the critical behavior of the compositional fluctuations. For these studies a sample of the zero-scattering alloy $^{62}Ni_{42.7}{}^{63}Cu_{57.3}$ was used. As discussed before, this allows for the direct measurement of S_{CC}. For these studies special care was taken in optimizing the shielding of the primary beam behind the sample, which allowed us to slightly increase the accessible range of momentum transfer to smaller q-values as compared to our former measurements. Figure 6 shows temperature dependence of S_{CC} at small momentum transfer. The increase of S_{CC} to small q gets slightly more pronounced if the temperature is decreased from 1670 K (above the liquidus temperature of

1560 K) to 1510 K (in the regime of an undercooled melt). This shows that the compositional fluctuations increase with decreasing temperatures. Nevertheless the variation of S_{CC} is too small to allow for quantitative analysis of the scaling behavior, possibly because the critical temperature is far below the experimentally accessible temperature regime.

4. Conclusions

In conclusion the neutron diffraction experiment on the zero scatterer $^{62}Ni_{42.7}{}^{63}Cu_{57.3}$ and isotopically substituted samples of the same composition have shown that Ni–Cu is not as conventionally assumed an ideal solution. Instead Ni–Cu shows some chemical short-range order as evidenced in the concentration–concentration structure factor $S_{CC}(q)$. In particular, the rise at low-q values points to a demixing behavior of Ni–Cu. This is in accordance with the slightly positive enthalpy of mixing reported previously. Interestingly, the experimental results found here for $Ni_{42.7}Cu_{57}$ are in good agreement with predictions from a simple generic model basing on Lennard–Jones potentials [21].

ORCID iDs

Dirk Holland-Moritz ⓘ https://orcid.org/0009-0000-2457-7427
Fan Yang ⓘ https://orcid.org/0000-0001-5281-2957
Florian Kargl ⓘ https://orcid.org/0000-0001-9902-0420

References

[1] Debenedetti P G, Sciortino F and Zerze G H 2000 *Science* **369** 289
[2] Mishima O 2010 *J. Chem. Phys.* **133** 144503
[3] Tanaka H, Kurita R and Mataki H 2004 *Phys. Rev. Lett.* **92** 025701
[4] Greaves G N *et al* 2008 *Science* **322** 566
[5] Munitz A and Abbaschian R 1996 *Metall. Mater. Trans.* A **27** 4049
[6] Gao J, Volkmann T, Roth S, Löser W and Herlach D M 2001 *J. Magn. Magn. Mater.* **234** 313
[7] Mattern N *et al* 2013 *Calphad* **42** 19

[8] Ruppersberg H and Knoll W 1977 *Z. Naturforsch.* A **32** 1374

[9] Katayama Y, Inamura Y, Mizutani T, Yamakata M, Utsumi W and Shimomuraor O 2004 *Science* **306** 848

[10] Mishima O, Takemura K and Aoki K 1991 *Science* **254** 406

[11] Koza M M, Geil B, Winkel K, Köhler C, Czeschka F, Scheuermann M, Schober H and Hansen T 2005 *Phys. Rev. Lett.* **94** 125506

[12] Koster W and Schule W 1957 *Z. Metallkd.* **48** 592

[13] Mozer B, Keating D T and Moss S C 1968 *Phys. Rev.* **175** 868

[14] Meijering J L 1957 *Acta Metall.* **5** 257

[15] Vrijen J and Radelaar S 1978 *Phys. Rev.* B **17** 409

[16] Chakrabarti D J, Laughlin D E, Chen S W and Chang Y A 1991 *Binary Alloy Phase Diagrams T B* Massalski (American Society for Metals, Metals Park OH)

[17] Richardsen T, Lohöfer G and Egry I 2002 *Int. J. Thermophys.* **23** 1207

[18] Takeuchi S and Endo H 1962 *Trans. Japan Inst. Met.* **3** 30

[19] Bhatia A B and Thornton D E 1970 *Phys. Rev.* B **2** 3004

[20] Stolz U K, Arpshofen I, Sommer F and Predel B 1993 *J. Phase Equilibria* **14** 473

[21] Amore S, Horbach J and Egry I 2011 *J. Chem. Phys.* **134** 044515

[22] Das S K, Horbach J, Binder K, Fisher M E and Sengers J V 2006 *J. Chem. Phys.* **125** 024506

[23] Holland-Moritz D, Schenk T, Convert P, Hansen T and Herlach D M 2005 *Meas. Sci. Technol.* **16** 372

[24] Holland-Moritz D, Stüber S, Hartmann H, Unruh T, Hansen T and Meyer A 2009 *Phys. Rev.* B **79** 064204

[25] Nowak B, Holland-Moritz D, Yang F, Voigtmann T, Kordel T, Hansen T C and Meyer A 2017 *Phys. Rev. Mater.* **1** 025603

[26] Nowak B, Holland-Moritz D, Yang F, Voigtmann T, Evenson Z, Hansen T C and Meyer A 2017 *Phys. Rev.* B **96** 054201

[27] Holland-Moritz D, Yang F, Gegner J, Hansen T, Ruiz-Martín M D and Meyer A 2014 *J. Appl. Phys.* **115** 203509

[28] Fischer H E, Barnes A C and Salmon P S 2006 *Rep. Prog. Phys.* **69** 233

[29] Holland-Moritz D, Heinen O, Bellissent R, Schenk T and Herlach D M 2006 *Int. J. Mat. Res.* **97** 947

[30] Faber T E and Ziman J M 1965 *Phil. Mag.* **11** 153

[31] Brillo J and Egry I 2003 *Int. J. Thermophys.* **24** 1155

[32] Schenk T, Holland-Moritz D, Simonet V, Bellissent R and Herlach D M 2002 *Phys. Rev. Lett.* **89** 075507

[33] Sachdev S and Nelson D R 1985 *Phys. Rev.* B **32** 1480

[34] Peng H L, Voigtmann T, Kolland G, Kobatake H and Brillo J 2015 *Phys. Rev.* B **92** 184201

[35] Brillo J and Egry I 2004 *Int. J. Mat. Res.* **95** 691